


CASE STUDY

Adaptive replanning using cone beam CT for deformation of original CT simulation

Casey Bojecho, PhD, Patricia Hua, CMD, Whitney Sumner, MD, Kripa Guram, MD, Todd Atwood, PhD, & Andrew Sharabi, MD, PhD 

Department of Radiation Medicine and Applied Sciences, University of California San Diego, La Jolla, California, USA

Keywords

Adaptive radiotherapy (ART) < radiation therapy, deformable registration < radiation therapy, general < discipline, head and neck < clinical site, medical imaging < general, palliative < general, radiotherapy (radiation therapy) < discipline

Correspondence

Andrew Sharabi, Department of Radiation Medicine & Applied Sciences, UC San Diego Health, 3855 Health Sciences Dr MC 0843, La Jolla, CA 92037, USA; Tel: +1 (858) 822-6040; Fax: 858-822-6081; E-mail: sharabi@ucsd.edu

Received: 5 January 2021; Revised: 16 August 2021; Accepted: 3 September 2021

J Med Radiat Sci **69** (2022) 267–272

doi: 10.1002/jmrs.549

Introduction

During the course of head-and-neck cancer treatment, anatomical changes such as tumour shrinkage and weight loss can result in significant plan deviations from the planning computed tomography (CT), including the planning target volume (PTV) extending into free space where there is no longer any tissue or tumour present. Correcting this plan deviation then requires repeating a CT simulation scan and replanning. This offline adaptive approach requires an additional CT simulation appointment and places additional stressors on patients, especially those with mobility issues. Additionally, it uses an additional CT simulation time slot which could delay a treatment start for new patient, especially in a busy radiation oncology clinic where CT simulation time slots are limited. Thus, it would be beneficial to find an alternative workflow to avoid the need to repeat a CT simulation for every adaptive replan.

Abstract

Background: During a course of radiation therapy, anatomical changes such as a decrease in tumour size or weight loss can trigger the need for repeating a computed tomography (CT) simulation scan in order to generate a new treatment plan. This adaptive approach requires a separate appointment for an additional CT scan which generates additional burden, cost, and radiation exposure for patients. **Case Presentation:** Here, we present a case of a head and neck cancer patient who required palliative radiation for a large neck mass. During treatment, he had a remarkable response which required a replan due to rapid tumour downsizing. In this case, we used a novel technique to avoid repeating the planning CT simulation by using a mid-treatment high-quality cone beam CT (CBCT) to deform the secondary image (plan CT) of the original planning CT and generate a new adapted treatment plan. **Conclusion:** This is the first report to our knowledge using a Halcyon CBCT to deform the original planning CT in order to generate a new radiation treatment plan, and this novel technique represents a new potential method of adaptive replanning for select patients.

Our department recently installed one of the first Halcyon (Varian Medical Systems, Palo Alto, CA) units in the USA. This Varian Halcyon has recently been equipped with a kilo-voltage imaging system that can perform cone beam CT (CBCT) with a field of view of up to 28 cm in the superior–inferior direction. This longitudinal field of view can encompass large head-and-neck tumours and is much larger than a TrueBeam, which is 17 cm for a head protocol. Additionally, the cone beam reconstruction algorithm uses a new iterative approach to provide improved soft tissue contrast.¹ While the CBCT scans available for the Halcyon provide improved image quality, the accuracy of the Hounsfield Units has not been assessed and therefore dose calculation on the CBCT could not be used for replanning at this time. However, the soft tissue contrast and low image noise in the CBCT allowed for an accurate deformable image registration. The initial planning CT was registered to the CBCT and then used for replanning,

removing the need to repeat patient CT simulation. Previous studies have used a similar approach; due to the limited longitudinal range of CBCT scans, the primary planning CT is required in regions outside of CBCT the field of view.² Due to the large field of view of the Halcyon, CBCT large head-and-neck tumours can be included in the field of view.

Here, we present a case where a palliative head-and-neck patient's body and tumour contour changed significantly due to mid-treatment tumour response. We obtained consent and permission from the patient for publication of his case and images. Due to his medical condition, the patient was unable to attend an additional CT simulation without requiring medical transport, as our CT simulator is housed in a different building than his treatment machine. Instead of proceeding with repeat planning CT simulation, a mid-treatment CBCT was used to perform a deformable image registration of the original planning CT, which was used to adaptively replan the treatment.

Case presentation

A 65-year-old male, after presenting to the emergency department, was diagnosed with (T0N3M0) squamous cell carcinoma of an unknown primary with a large fungating right neck mass. Figure 1A shows a photograph of the neck prior to treatment.

A CT with contrast demonstrated an 8.4 cm mass within the right neck extending from the level of the inferior oropharynx to the base of the neck. A positron emission tomography/computed tomography scan (PET/CT) demonstrated a large right neck mass, with a standardised uptake value maximum (SUV) of 17.5, a separate right posterior nasopharyngeal mass (SUV 15.8), and a small focus of prominent uptake in the right aspect of the sphenoid sinus (SUV 5.5).

The patient was experiencing severe pain and pressure sensation in the neck with decreased range of motion, as well as loss of appetite and decreased energy. The patient was only able to tolerate some liquids orally, and a feeding tube was placed after the first fraction of radiation therapy.

Palliative radiation therapy of 50 Gy in 20 fractions (2.5 Gy/fraction) was prescribed to help improve his symptoms. In order to accommodate this dose escalation while minimising toxicity, the patient was treated with volumetric modulated arc therapy. The planning CT was taken on a GE Discovery CT590 (General Electric, Boston MA), with 120 kVp, a scan length of 45.25 cm with a slice thickness of 0.25 cm (181 slices). The planning target volume had a maximum length of 15.39 cm superior–inferior, 10.96 cm anterior–posterior, 8.81 left–right, and a volume of 660 cm.³

The dose constraints for planning followed our institutional guidelines and were generated using our institution's Eclipse RapidPlan head-and-neck model. The submandibular and parotid gland had a mean constraint of 26 Gy. The mean dose constraint of the larynx was below 40 Gy, and the mean of the pharynx, larynx, and oesophagus is less than 45 Gy. The spinal cord had a maximum dose limit of 50 Gy. Due to the proximity to the PTV, the ipsilateral submandibular constraint was exceeded. All other constraints were met with dose kept as low as possible.

For patient setup, a CBCT was performed prior to every fraction, aligning to boney anatomy. Over the course of several fractions, tumour shrinkage was observed on the CBCT, and after 10 fractions of treatment a decision was made to replan.

The patient was unable to attend a planning CT scan without ambulance transport. Given the high quality of the CBCT images, the alternative strategy of deforming the planning CT to the CBCT was investigated.

On the 10th fraction of treatment, the patient had a CBCT, 24.6 cm in length, extending inferior to the clavicle and superior to the eyes. Figure 2 shows the sagittal view of the CBCT. The scanning region encapsulated the entire target extending beyond the planning target volume by 3.5 cm superiorly and 5.1 cm inferiorly.

The original planning CT scan, taken 36 days prior, was registered to the CBCT, using the VoxAlign deformable image registration algorithm in MIM (MIM Maestro, Cleveland OH). The workflow in MIM begins with a rigid registration, followed by an intensity-based free-form deformable registration. The algorithm uses a course-to-fine multi-resolution approach to define a grid of control points. The optimisation strategy is a custom-modified gradient descent. The deformed CT is cropped to the length of the CBCT scan.

The registration deformed the CT Hounsfield units and planning structures. The deformable registration was reviewed by a physicist using the “Reg Revel” tool, to ensure local registrations agreed at points throughout the scan. Additionally, it was verified that the visible boundaries of anatomy were well aligned with contours. The structure volumes from the original planning CT and the deformed planning CT were compared. The deformed contours were reviewed by the oncologist for accuracy. The volume of the PTV was reduced by 16% (660.1 – 552.0 cc), the left parotid adjacent to the tumour changed by 23% (23.2–17.8 cc), and the right parotid changed by 13% (27.1–23.4 cc). For all other organs at risk, the volume changed by less than 5%. The digital bolus was modified to better match the CBCT. For all fractions of treatment, the bolus was placed on the outside of a



Figure 1. Photographs taken (A) Pre-treatment, (B–C) during treatment and (D) one month post-treatment.

thermoplastic mask. For the PTV and organ at risk structures, the average HU before and after deformation was checked to ensure the deformation was not producing any spurious HU values that could affect the plan; for all structures with an optimisation objective, the mean HU value varied by 12 HU or less. A new plan was made using our institution's Eclipse RapidPlan head-and-neck model. The prescription dose covered 95% of the PTV volume for the adapted plan. The new contours, PTV, and plan were reviewed and accepted by the radiation oncologist with the remaining 10 fractions treated using the new plan.

Figure 3 shows the original plan on the planning scan (A), the planning CT deformed to the CBCT taken on the 10th fraction of treatment, with the original plan calculated, (B) the planning CT deformed to the CBCT taken on the 10th fraction of treatment, with the new adapted plan calculated, (C) the red arrow shows the plan deviation and PTV in free space due to tumour

downsizing during treatment course. For comparison, Figure 1B, C shows a photograph of the patient's neck during treatment. An estimate of the impact of not performing the adaptive replan is shown in Table 1. Shown are the mean and max dose (Gy) for the i) original plan for 20 fractions calculated on the original scan, ii) the original plan computed for 10 fractions on the original scan and 10 fractions on the CT deformed to the CBCT, and iii) the original plan computed for 10 fractions plan on the original scan added to the replan computed for 10 fractions on the CT deformed to the CBCT. Also shown is the percent difference between plans ii) and iii), showing a reduction in dose for every organ except the spinal cord. Dose calculations of the original plan and replan were performed in Eclipse.

At the end of treatment, the patient reported decreased pain and improved neck mobility and was able to tolerate more foods orally. The patient experienced moderate mucositis and skin erythema of the right neck. The

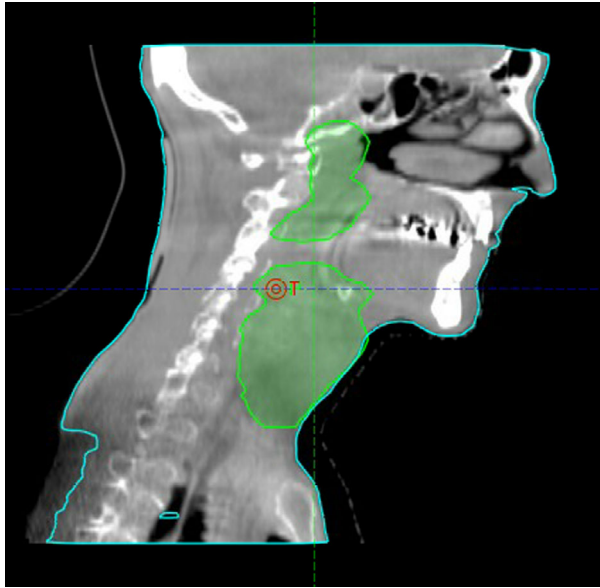


Figure 2. Sagittal view of CBCT taken on the 10th fraction.

Discussion and Conclusion

To our knowledge, this is the first report to successfully use a Halcyon extended FOV CBCT to deform a planning CT to replan a head-and-neck treatment adaptively. A previous retrospective study used a similar workflow to assess the ability of deforming Halcyon CBCT scans to assess margins for prostate treatments.³ Other retrospective studies have assessed the feasibility of using deformable registration to a CBCT to replan head-and-neck plans and found limitations in the field of view and soft tissue contrast.^{2,4} Previously, the limited field of view of CBCT has made the images unusable for treatment planning due to missing patient anatomy,⁵ and deforming the target volumes has been discouraged due to the lack of soft tissue contrast and target visibility. Additionally, the registration of CT to CBCT can be adversely affected by artefacts that are more likely to occur on the CBCT.⁶

The challenges listed above have been overcome by the large field of view of the kV imaging system and enhanced soft tissue contrast from the iterative CBCT

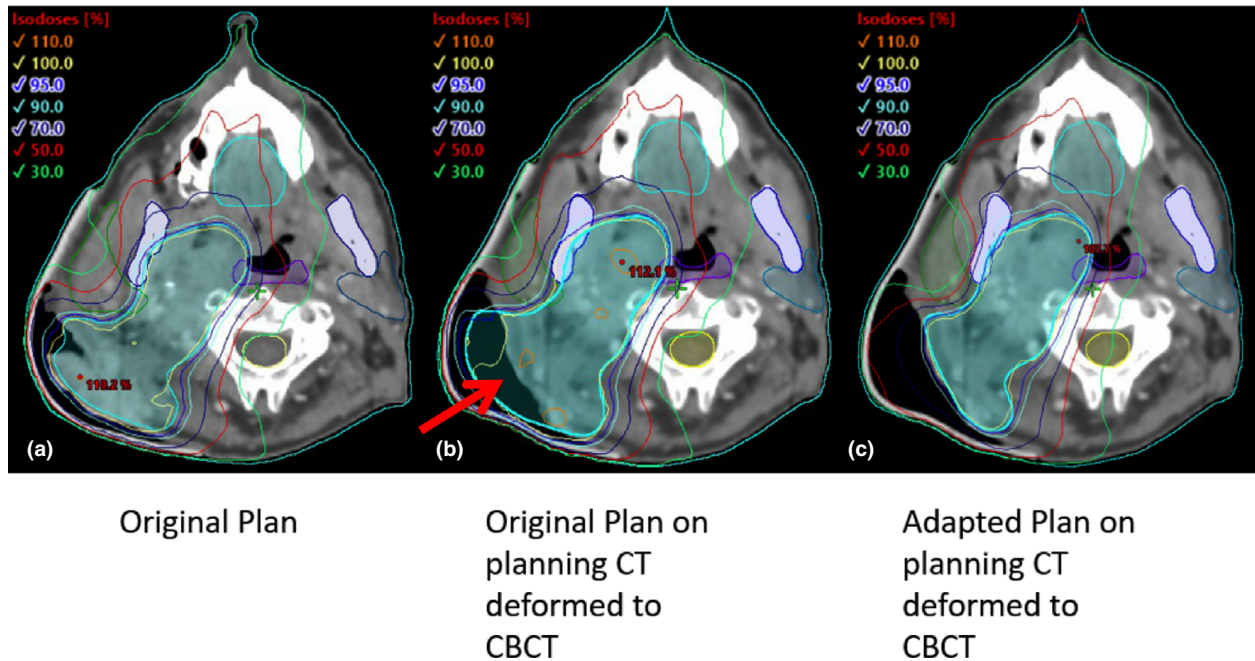


Figure 3. Axial view of original planning CT shown with original planning target volume (A), the planning CT deformed to the CBCT taken on the 10th fraction of treatment, with the original plan recalculated (B), the planning CT deformed to the CBCT taken on the 10th fraction with the replan calculated.

patient was seen at one-month follow-up and reported being pain free with normal range of motion and was noted to have a complete clinical response. Figure 1D shows a photograph of the patient's neck at one-month follow-up.

image reconstruction.⁷ The large field of view of the scan includes all relevant patient anatomy and the enhanced soft tissue contrast allows for reliable deformation of the planning CT as well as the organ at risk and target structures. The deformable registration approach with the

Table 1. Mean and maximum dose (Gy) for the original plan for 20 fractions calculated on the original scan, the original plan computed for 10 fractions on the original scan and 10 fractions on the CT deformed to the CBCT, and the original plan computed for 10 fractions plan on the original scan added to the replan computed for 10 fractions on the CT deformed to the CBCT.

Organ/Target	Original Plan: 20 fx calculated on original scan		Original Plan: 10 fx calculated on original scan and 10fx calculated on deformed CT		Original plan: 10 fx calculated of original scan and 10 fx re- plan calculated on deformed CT.		% Change between original plan versus re-plan on deformed CT versus	
	mean (Gy)	max (Gy)	mean	max	mean	max	mean	max
Oesophagus	9.22	31.69	10.90	34.26	9.09	29.10	-19.9	-17.8
Larynx	27.82	53.05	30.97	53.78	26.83	52.65	-15.4	-2.1
Oral cavity	25.63	42.45	25.72	44.38	24.63	42.61	-4.4	-4.2
Parotid left	7.22	12.62	7.24	11.95	6.03	11.96	-20.0	0.0
Parotid right	25.36	51.62	27.44	5.33	21.05	51.32	-30.4	-3.9
Pharynx	31.25	54.82	31.08	54.8	29.20	53.87	-6.4	-1.7
Spinal cord	12.41	18.86	12.93	19.31	14.19	21.87	8.9	11.7
Submandibular left	18.33	24.75	19.60	25.74	14.65	19.95	-33.8	-29.0
Submandibular right	48.23	51.93	51.94	53.39	49.61	52.27	-4.7	-2.1
Trachea	16.35	52.77	20.63	53.72	17.78	52.53	-16.0	-2.3
PTV	51.91	56.02	52.39	55.58	51.70	54.21	-1.3	-2.5

use of automated treatment planning with RapidPlan allowed for an adaptive replan that was much quicker than the conventional approach.

Previous head-and-neck studies have estimated the accuracy of calculating dose on a deformed CT to be within 2%.⁴ As an estimate of the impact of not performing the adaptive replan, the original plan was calculated on the deformed CT. Had the original plan been delivered for all 20 fractions, it would have resulted in significantly higher mean doses for the organs at risk; 34% for the left submandibular, 5% for the right submandibular, 20% for the left parotid, 30% for the right parotid, 15% for the larynx, 20% for the oesophagus, and 16% for the trachea. This is expected due to the tumour volume shrinking leading to the original plan over-covering the target, a result that has been well established in prior studies.^{6,8} Of note we did observe a slight increase in the spinal cord dose with this replan, indicating that additional quality control techniques and planning strategies need to be implemented to improve adaptive re-planning.

This case highlights the utility of a CBCT with a large field of view and improved soft tissue contrast for head-and-neck replanning. It is common for many tumour types including head-and-neck cancers, lung cancers, cervical cancers, and other tumour types to have marked tumour responses observed during treatment. Thus, this CBCT-based replanning strategy could be applied to other disease sites. However, there are obvious limitations to this approach such as cases where the immobilisation or thermoplastic

mask needs to be recreated or refitted. Before generalising the technique to include more patients, a more in-depth quality assurance of deformable image registration, using digital phantom test cases in accordance with TG-132,⁹ will be performed. Additionally, clinical protocols outlining the required patient-specific QA will be created for the efficient evaluation of future cases.

Repeating a CT simulation appointment can add additional time, burden, overhead cost, and scheduling challenges for radiation therapy patients. The CBCT-based replanning technique was used to quickly adapt and replan a palliative treatment plan with minimal burden to the patient and should be investigated further as our on-board imaging modalities continue to improve. In combination with automated planning algorithms, this technology shows promise in providing highly accurate and expeditious offline plan adaptation.

Competing Interests

A.B.S. reports research funding and honoraria from Pfizer and Varian Medical Systems, consultant fees from Astrazeneca, and Merck; A.B.S. is the scientific founder and has an equity interest in Toragen Inc. unrelated to the current work.

Funding

This work was supported in part by 1KL2TR001444 and San Diego Center for Precision Immunotherapy Grant.

References

1. Iterative Cone-Beam CT Improved visualization of soft tissue structures. 2017. https://www.varian.com/sites/default/files/resource_attachments/IterativeCBCTBrief_RAD104.pdf.
2. Hay LK, Paterson C, McLoone P, et al. Analysis of dose using CBCT and synthetic CT during head and neck radiotherapy: A single centre feasibility study. *Tech. Innov. Patient Support Radiat. Oncol* 2020; **14**: 21–9.
3. Studenski MT, Delgadillo R, Xu Y, et al. Margin verification for hypofractionated prostate radiotherapy using a novel dose accumulation workflow and iterative CBCT. *Phys. Medica* 2020; **77**: 154–9.
4. Veiga C, McClelland J, Moinuddin S, et al. Toward adaptive radiotherapy for head and neck patients: Feasibility study on using CT-to-CBCT deformable registration for ‘dose of the day’ calculations. *Med Phys* 2014; **41**(3): 31703.
5. Ding GX, Duggan DM, Coffey CW, et al. A study on adaptive IMRT treatment planning using kV cone-beam CT. *Radiother Oncol* 2007; **85**(1): 116–25.
6. Tsuji SY, Hwang A, Weinberg V, Yom SS, Quivey JM, Xia P. Dosimetric evaluation of automatic segmentation for adaptive IMRT for head-and-neck cancer. *Int J Radiat Oncol Biol Phys* 2010; **77**(3): 707–14.
7. Gardner SJ, Mao W, Liu C, et al. Improvements in CBCT image quality using a novel iterative reconstruction algorithm: A clinical evaluation. *Adv. Radiat. Oncol* 2019; **4**(2): 390–400.
8. Surucu M, Shah KK, Roeske JC, Choi M, Small W, Emami B. Adaptive radiotherapy for head and neck cancer: Implications for clinical and dosimetry outcomes. *Technol. Cancer Res. Treat* 2017; **16**(2): 218–23.
9. Brock KK, Mutic S, McNutt TR, Li H, Kessler ML. Use of image registration and fusion algorithms and techniques in radiotherapy: Report of the AAPM Radiation Therapy Committee Task Group. *Med Phys* 2017; **44**(7): e43–76.